Barriga, F.J.A.S., Binns, R.A., Miller, D.J., and Herzig, P.M. (Eds.)
Proceedings of the Ocean Drilling Program, Scientific Results Volume 193

13. Core-Scale Permeability of an Actively Venting, Felsic-Hosted Hydrothermal System: the PACMANUS Hydrothermal Field[1]

L.B. Christiansen[2] and G.J. Iturrino[3]

ABSTRACT

Permeability of the ocean crust is one of the most crucial parameters for constraining submarine fluid flow systems. Active hydrothermal fields are dynamic areas where fluid flow strongly affects the geochemistry and biology of the surrounding environment. There have been few permeability measurements in these regions, especially in felsic-hosted hydrothermal systems. We present a data set of 38 permeability and porosity measurements from the PACMANUS hydrothermal field, an actively venting, felsic hydrothermal field in the eastern Manus Basin. Permeability was measured using a complex transient method on 2.54-cm minicores. Permeability varies greatly between the samples, spanning over five orders of magnitude. Permeability decreases with both depth and decreasing porosity. When the alteration intensity of individual samples is considered, relationships between depth and porosity and permeability become more clearly defined. For incompletely altered samples (defined as >5% fresh rock), permeability and porosity are constant with depth. For completely altered samples (defined as <5% fresh rock), permeability and porosity decrease with depth. On average, the permeability values from the PACMANUS hydrothermal field are greater than those in other submarine environments using similar core-scale laboratory measurements; the average permeability, 4.5×10^{-16} m^2, is two to four orders of magnitude greater than in other areas. Although the core-scale permeability is higher than in other seafloor environments, it is still too low to obtain the fluid ve-

[1]Christiansen, L.B., and Iturrino, G.J., 2004. Core-scale permeability of an actively venting, felsic-hosted hydrothermal system: the PACMANUS hydrothermal field. *In* Barriga, F.J.A.S., Binns, R.A., Miller, D.J., and Herzig, P.M. (Eds.), *Proc. ODP, Sci. Results,* 193, 1–19 [Online]. Available from World Wide Web: <http://www-odp.tamu.edu/publications/193_SR/VOLUME/CHAPTERS/202.PDF>. [Cited YYYY-MM-DD]
[2]U.S. Geological Survey, 345 Middlefield Road, MS 421, Menlo Park CA 94025, USA. lchristi@usgs.gov
[3]Borehole Research Group, Lamont-Doherty Earth Observatory, Columbia University, PO Box 1000, 61 Route 9W, Palisades NY 10964, USA.

Initial receipt: 4 May 2003
Acceptance: 18 June 2004
Web publication: 1 September 2004
Ms 193SR-202

locities observed in the PACMANUS hydrothermal field based on simplified analytical calculations. It is likely that core-scale permeability measurements are not representative of bulk rock permeability of the hydrothermal system overall, and that the latter is predominantly fracture controlled.

INTRODUCTION

Large-scale fluid circulation in the oceanic crust is known to be important in controlling hydrothermal and geochemical processes in a variety of geophysical settings. In some active spreading centers, hydrothermal fluid flow is thought to be a natural analog of ancient ore-forming systems for massive sulfides. In order to produce these ore deposits, large volumes of fluid must circulate through the system, requiring high permeabilities inherent in porous and fractured lavas (Fisher, 1998). In the Manus Basin, located behind an active island arc near Papua New Guinea, volcanic-hosted massive sulfide deposits are currently forming (Fig. F1). Because felsic volcanic host rocks dominate the PACMANUS hydrothermal field, it offers a modern analog for ancient volcanic-hosted massive sulfide deposits (Binns and Scott, 1993).

F1. Location of the PACMANUS hydrothermal field, p. 11.

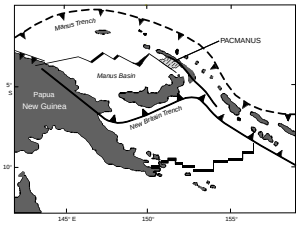

Intrinsic permeability plays an integral factor in controlling the fluid flow patterns that determine the spatial distribution, lateral extent, and concentration of ore deposits. Previous studies of active hydrothermal systems examined basalt-hosted and sediment-hosted mineralized settings. Leg 193 of the Ocean Drilling Program (ODP) at PACMANUS undertook the first drilling of a felsic volcanic-hosted system, providing new data regarding the physical properties and alteration features of volcanic rock from this complex hydrothermal environment. Here we present an analysis of core-scale permeability and porosity measurements of felsic volcanic rock samples from the actively venting PACMANUS hydrothermal field and compare them to rock characteristics. Permeability data can be used to help interpret the nature of fluid flow in the region and to understand the impact of hydrothermal flow on the ore-forming process.

GEOLOGIC SETTING

The PACMANUS hydrothermal field in the eastern Manus Basin is a site hosted by felsic lavas (Binns and Scott, 1993; Yang and Scott, 1996), with extensive subsurface alteration (Binns, Barriga, Miller, et al., 2002). The hydrothermal vent field lies near the bathymetric peak of a high-standing, 20-km-long Y-shaped ridge, called the Pual Ridge (Binns and Scott, 1993). The Pual Ridge and the PACMANUS site are composed of felsic volcanic lavas, ranging from andesite to rhyodacite (Binns et al., 1995). Discontinuous hydrothermal deposits were viewed from camera tows throughout a 3-km × 800-m zone along the Pual Ridge, displaying chimney deposits up to 20 m high (Binns, Barriga, Miller, et al., 2002). In addition to chimney deposits, thin blue-gray crusts associated with white patches (interpreted as bacterial mats) indicate potential hydrothermal deposits produced by low-temperature discharge. The polymetallic sulfide deposits, which are rich in copper, zinc, lead, silver, and gold, are derived from seawater–rock interactions, with possible mixing of magmatic fluids (Yang and Scott, 1996).

Permeability measurements were made on samples from three locations: Snowcap (Holes 1188A and 1188F), Roman Ruins (Holes 1189A and 1189B), and Satanic Mills (Hole 1191A). Snowcap is an area of extensive diffusive venting with low-temperature hydrothermal fluids. The mineralization and hydrothermal alteration patterns extend to the bottom of the cored interval at ~387 meters below seafloor (mbsf). However, there are no significant developments of massive base metal sulfides or precious metal enrichments in the recovered sections. Roman Ruins is the most developed area of active sulfide–sulfate chimneys in the PACMANUS hydrothermal field, with chimneys as tall as 20 m, though averaging 3 m (Binns, Barriga, Miller et al., 2002). Hole 1189A was drilled to a depth of ~126 mbsf, and Hole 1189B was drilled to 206 mbsf. Although Holes 1189A and 1189B were in close proximity (~35 m), variations between Holes 1189A and 1189B in the recovered intervals are quite large, with a possible stockwork zone intersected in Hole 1189B. Satanic Mills is a chimney field with high-temperature fluid discharge covered by a hard, vesicular dacite/rhyodacite crust, as found at the other sites. Early collapse of the hole limited the depth of drilling to ~20 mbsf; however, drilling did provide samples of the hard crust layer. The samples taken from this region provided permeability information about the less altered volcanics found near the surface.

METHODOLOGY

Laboratory permeability and porosity measurements were made at New England Research, Inc. (NER). Tests were conducted on 2.54-cm diameter minicores, with lengths ranging from 1 to 3.5 cm. All minicore samples were extracted perpendicular to the orientation of the recovered drill core. Details of drilling procedures, core recovery, and minicore extraction are described in Binns, Barriga, Miller, et al. (2002). Permeability measurements were made along the length of the minicores; therefore, the resultant permeability values represent fluid flow along the horizontal axis. No vertical permeability measurements were made because of the limitations in the amount of core recovered. Also, no permeability measurements were made on incoherent material because of the nature of the sampling and measurement procedures; only coherent rock was used for our testing purposes. Samples were selected from depths ranging from 9 to 372 mbsf, with a water depth of ~1675 m (varying between holes). Samples represent the majority of the cored intervals and characterize the primary lithologic units and alteration intensities found in the recovered core, as classified by shipboard analysis. Although there may be some sample bias of the overall system because of limited core recovery (ranging from 0% to 20%, and below 10% on average) (Binns, Barriga, Miller, et al., 2002) and the inability to sample structurally fragmented rock, the sample selections reflect as many of the recovered rock types as possible.

Samples were saturated with 31 g/L sea salt solution using “sea salt” produced by Sigma Chemical Co. for 48 hr prior to permeability testing to saturate the samples. A brine solution representative of seawater was used for saturation as well as for permeability tests to better replicate submarine conditions and to give more reliable results. If gas were used instead of salt water, measurement time could be reduced; however, the possibility of interactions between the salt water and clay minerals could be significant for fluid flow (Karato, 1983a). Because anhydrite was identified in a number of samples and saturation could cause anhy-

drite dissolution, the saturation fluid was analyzed after the 48-hr period to determine if any minerals present in the sample had dissolved. In all cases, the amount of additional Ca and SO_4 detected in the solution was insignificant, and anhydrite dissolution in the samples was determined to have no effect on the permeability or porosity measurements. Porosity was inferred from the difference between the saturated and dry densities for each sample, similar to the shipboard technique employed by ODP. Based on the reproducibility of measurements, errors in porosity estimates are on the order of ±0.2 porosity units (p.u.) (i.e., ±0.2%). Other sources of measurement error, such as irregular sample geometry, were negligible for these samples. Two samples, 193-1189A-2R-1, 8–11 cm, and 2R-1, 36–38 cm, exhibited large surface pores which tend to drain prior to weighing, leading to systematic underestimates of porosity. Based on historical results, these errors are generally found to be <1 p.u. (G. Boitnott, pers. comm., 2003).

For each sample, the ends were polished flat and parallel to fit properly in the core holder. The samples were placed between two porous steel frits, which uniformly distributed the fluid flow and stress. All permeability measurements were made at room temperature. Permeability was measured with a complex transient method, using the equipment and technique described in Boitnott (1997). In this method, permeability is measured by applying a pressure perturbation to the pore pressure field at the upstream end of the sample and measuring the pressure response at the downstream end. By using a variety of transient frequencies as perturbations, the signal can be optimized while maintaining measurement accuracy. A single-frequency sinusoid was used in most cases, tuned to optimize the signal for each sample. An asymmetrical spike transient was used for higher-permeability samples, whereas a traditional step function (pulse decay) was used for lower-permeability samples.

Permeability was first measured under 5-MPa effective pressure (confining pressure = 10 MPa; pore pressure = 5 MPa). The effective pressure was increased to 50 MPa for each sample and then reduced again to 5 MPa; permeability measurements were made at each 5-MPa interval. After each step increase or decrease in pressure, pore pressure was permitted to reequilibrate. In some cases, particularly for softer, lower-permeability samples, the reequilibration time period was long, with tests taking >1 week to complete. Errors in permeability measurements are difficult to generalize and quantify. Variability between measurements using different transients generally resulted in discrepancies of <5%. By fitting data assuming a wide range of specific storages, errors resulting from uncertainties in specific storage are thought to be less than ±10%. Through a direct comparison of measured transient and steady-state permeabilities on selected samples spanning a wide permeability range, measurement discrepancies greater than ±30% were observed (G. Boitnott, pers. comm., 2003).

RESULTS

Permeabilities are reported at effective pressures of 15 MPa. For the majority of the samples, pressure had little effect on the results of the measurements (Fig. F2). For these samples, permeability was relatively constant over the span of the test, both with pressure increases and decreases. Several samples did respond to pressure changes, with permeability decreasing as pressure increased (Fig. F3). For most of this subset

F2. Permeability measurements for samples with little response to pressure, p. 12.

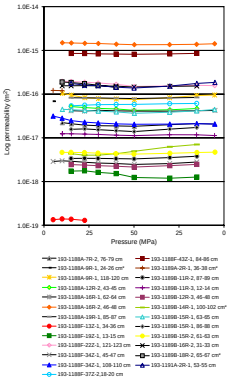

F3. Permeability measurements for samples with a large response to pressure, p. 13.

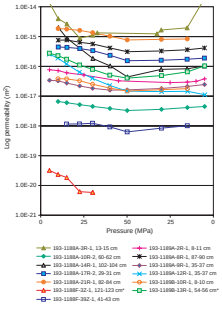

of samples, the permeability change was <50%; however, for five samples the change in permeability was close to or greater than an order of magnitude (Samples 193-1188A-3R-1, 13–15 cm; 193-1189A-12R-1, 35–37 cm; 193-1188A-14R-1, 102–104 cm; 193-1188F-3Z-2, 121–123 cm; and 193-1189B-13R-1, 54–56 cm). The decrease in permeability is likely caused by a reduction of interconnected pore space caused by the increase in pressure. The latter three samples were damaged during the testing procedure, which would contribute to the decrease in measured permeability. The variation in the response to pressure change between the samples may be dependent on the lithology, amount, or style of alteration; the amount of interconnected porosity; or a combination or factors. It may be noted that all of the complete measurements from Hole 1189A decreased with increasing pressure. However, there is no petrological data from the samples to determine the cause of the differences. Many of the samples affected by pressure changes did not regain permeability as pressure was decreased (i.e., Samples 193-1188A-21R-1, 82–84 cm). This may be because of structural degradation induced by the high pressures used in the measurement process.

Six samples were damaged during testing due to collapse or compaction that caused a permanent reduction in permeability before a reliable measurement could be made. Although we are not confident in the measurements for these samples, they are included in the following graphs and marked as damaged. Values for these samples are not included in the discussion of the results. Damage to the samples occurred during permeability testing, which was made after the porosity calculations; therefore, all porosity values are representative of the samples. Regardless, samples are marked as damaged in both porosity and permeability plots for consistency.

Both permeability and porosity measurements of the samples were highly variable between samples. Permeabilities measured in reliable tests ranged from ~1.4×10^{-19} to 7.0×10^{-15} m² (Table T1), with an average of 4.5×10^{-16} m². Broadly, permeability decreases with depth, but with considerable scatter of the core-scale measurements (Fig. F4). Permeability values are more tightly grouped near the seafloor and become more scattered as depth increases. Correlations to other physical properties, such as thermal conductivity, velocity, vesicularity, composition, or grain density, are weak if present. Qualitative examinations of thin sections from a subset of the minicore samples (samples with compositional analyses in Table T1) indicate that microscopic features such as crystal size and structural fabric also do not have obvious correlations to the permeability.

Porosity values calculated at NER vary from ~1% to 43% (Fig. F5), with an average of 21%. Values calculated at NER are similar to shipboard measurements, which ranged from <1% to 47% for the same sample set. Permeability decreases with decreasing porosity (Fig. F5), although at midrange porosities and permeabilities the values are more scattered. The one low porosity, high permeability sample is from ~372 mbsf and has 26% relict plagioclase based on thin section analysis, indicating that it is much less altered than other samples of similar depth.

DISCUSSION

When the alteration intensity is considered, the correlations between depth and both porosity and permeability are more clearly defined (Fig. F6). Alteration intensity is categorized as fresh (<2% alteration), slight

T1. Physical properties of samples, p. 19.

F4. Permeability vs. depth, p. 14.

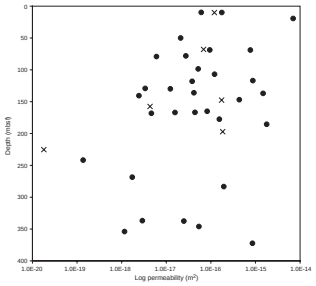

F5. Permeability vs. porosity, p. 15.

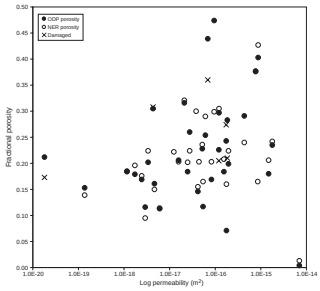

F6. Porosity and permeability vs. depth, p. 16.

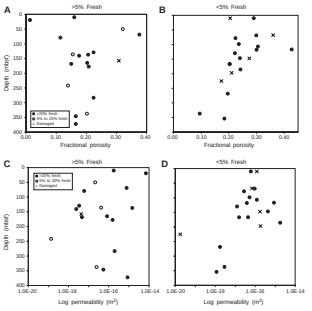

(2%–10% alteration), moderate (10%–40% alteration), high (40%–80% alteration), very high (80%–95% alteration), and complete (95%–100% alteration), following the classification system described in Binns, Barriga, Miller, et al. (2002). Alteration intensities and mineral compositions listed in Table **T1** are from shipboard analyses of thin sections when available. Thin sections are coincident with samples, except where noted in Table **T1.** For samples without corresponding thin section analyses, alteration intensity is based on alteration logs and graphic logs of the core (Binns, Barriga, and Miller, et al., 2002), and modified using the same criteria and techniques to better characterize the sample because heterogeneities exist within many described rock sections. Unaltered materials, termed fresh for the remainder of this paper, include relict plagioclase, pyroxene, and glass.

In samples with >5% fresh material (all samples not completely altered), porosity is relatively constant with depth (Fig. **F6A**). With the exception of four outliers, porosity ranges from 11% to 22%. The sample with the lowest porosity, 1%, is a fresh sample from the top portion of Hole 1188A. The three porosity values that are significantly higher than the rest of the samples come from samples that exhibit clastic or hydrothermal breccia textures and flow banding. The only other clastic sample in this suite is the very highly altered sample at 337.48 mbsf, with a midrange porosity of 20%. The clastic nature of the rock could allow higher void space in the rock structure; however, it is not reflected by an increase in permeability. In samples with <5% fresh material, porosity decreases with depth, from ~30% near the seafloor to 15% at ~350 mbsf (Fig. **F6B**). The maximum porosity measurement was 42% at 117 mbsf, and the minimum was 10% at 336 mbsf. The decrease in porosity corresponds to an increase in the amount of quartz with depth and a disappearance of cristobalite by ~130 mbsf, especially apparent at Site 1188. Both cristobalite at upper levels and quartz at depth can fill void spaces, such as vesicles, so the decrease in porosity with depth is likely related to the crystallization of quartz in the body of the rocks.

Permeability measurements are more variable with depth. For samples with >5% fresh material, permeability generally remains constant with depth (Fig. **F6C**). Permeability in the majority of samples ranges from 10^{-18} to 10^{-15} m². One sample with a high permeability value of 6.99×10^{-15} m², located at 19.36 mbsf, is a fresh rock from the uppermost section of Hole 1188A with <10% alteration. The outlying low-permeability sample, 1.37×10^{-19} m², at 241 mbsf, is a very highly altered sample with only 7% fresh material. This sample seems to better fit the trend of completely altered samples. In completely altered samples, permeability gradually decreases with increasing depth, similar to the trend seen in the porosity-depth profile for completely altered samples. Values range from ~10^{-16} m² near the seafloor to ~10^{-18} m² below 300 mbsf (Fig **F6D**). One slightly higher permeability value at 185 mbsf of ~10^{-15} m² is from a large silica-magnetite vein, which may contribute to the higher permeability value; however, it is not reflected by the porosity.

When porosity–permeability relationships are considered for subsets of data based on the amount of alteration, the correlation between permeability and porosity is stronger (Fig. **F7**). For samples with >5% fresh material, there is no obvious trend between porosity and permeability. Values are generally clustered in the middle range for both permeability and porosity, with several outlying data points. For completely altered samples, there is a defined correlation between porosity and depth, in which permeability decreases with decreasing porosity. In completely

F7. Porosity vs. permeability, p. 17.

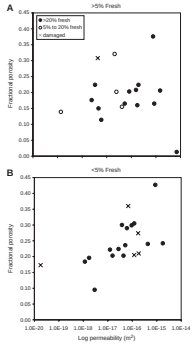

altered samples, both the permeability and porosity are similarly affected. One possible explanation for the correlation found in altered samples is that the formation of alteration products and subsequent removal of igneous minerals causes the porosity and permeability to be solely dependent on alteration. With less altered samples, more of the relict texture remains in the rock, which can be more variable, thus creating a more scattered permeability–porosity relationship.

The mean value of permeability measurements from the PACMANUS hydrothermal field is significantly greater than in other submarine environments at the core scale (Fig. F8). As compared to samples from both young and old crust in a variety of geophysical settings (Johnson, 1980; Karato, 1983a, 1983b; Christensen and Ramananantoandro, 1988; Iturrino et al., 2000), the average permeability is two to four orders of magnitude greater than in other regions. A fundamental difference between the samples in this study and those of other seafloor environments is that samples from the PACMANUS basin are felsic rocks and in most cases are extremely altered. It is possible that felsic rocks are inherently more permeable or that the alteration process could increase permeability within rocks. However, less altered samples did not have significantly lower permeabilities than completely altered samples. Moreover, the only fresh sample in this study had the highest permeability. While this hints that some characteristic like vesicularity in felsic rocks contributes to the higher permeability, the data provide no clear indication of the relative roles of alteration and precursor rock type.

F8. Comparison of core-scale permeability, p. 18.

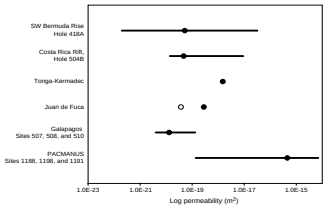

Although surface fluid venting is quite different between Sites 1188, 1189, and 1191, permeability measurements do not vary systematically between holes. Site 1189, which exhibits the most vigorous flow at chimneys, has core-scale permeability values ranging from 3.37×10^{-18} to 7.69×10^{-16} m². This range is similar to that of Site 1188, where flow at the seabed is only diffuse, in which permeability varies from 1.37×10^{-19} to 6.99×10^{-15} m². Because surface fluid flow at the two contrasted sites is not reflected in the core-scale permeabilities, other factors must exert the dominant control.

Core-scale measurements do not include the impacts of larger regional features, such as faulting and macro-scale fractures. We can use a simplified, one-dimensional analytical model to estimate the likely fluid flow velocities in a medium with an isotropic, homogeneous permeability of 10^{-16} m². We can then compare the calculated value to observed velocities in the PACMANUS hydrothermal field to determine if fracturing is necessary to obtain the observed velocities. Assuming that the only driving force for fluid flow is buoyancy, pressure is hydrostatic, and fluid flow is in the vertical direction, fluid flow velocity (Darcy velocity = q) can be calculated using a modified version of Darcy's law (Domenico and Schwartz, 1997):

$$q = -(kg\rho_o\alpha\Delta T/\mu), \quad (1)$$

where

k = permeability,
g = gravity,
ρ_o = reference density for seawater,
α = thermal expansivity for seawater,

ΔT = difference in temperature between the bottom of a given borehole and the seafloor surface, and
μ = fluid viscosity.

In the deepest hole drilled during Leg 193, Hole 1188F, temperature measurements made using an ultra high temperature multisensor memory tool (UHT-MSM) temperature probe recorded a maximum temperature of 313°C at a maximum depth of 387 mbsf. Using a maximum ΔT of 313°C and fluid properties integrated over the range of pressures and temperatures along the flow path, the maximum Darcy velocity is <2 cm/yr. Although flow rates of venting fluids have not been rigorously measured in the PACMANUS hydrothermal field, estimates of flow rates at particular chimney orifices are in the range of 2–5 cm/s (R. Binns, pers. comm., 2003). Thus, with a bulk rock permeability of 10^{-16} m^2, the hydrothermal venting observed in the PACMANUS Basin could not occur.

In order to drive the rapid fluid flow observed in the PACMANUS hydrothermal field and produce chimney structures, particularly evident at the Roman Ruins site, there would likely be a mechanism to focus flow through more permeable zones. A likely fluid flow scenario would channel fluid through large-scale fractures, as seen in the Juan de Fuca Basin. For example, the one laboratory permeability measurement in basaltic rock from Middle Valley, Juan de Fuca Ridge, is up to six orders of magnitude less than that observed in in situ measurements, measured using packer testing (Becker et al., 1994; Iturrino et al., 2000). These results suggest that high-permeability zones are associated with fractures or faults (Iturrino et al., 2000), whereas the rock matrix has a significantly lower permeability. Similar hydrogeologic conditions may exist in the PACMANUS hydrothermal field; however, because of the nature and instability of the submarine environment, in situ permeability measurements were not possible during ODP Leg 193. Fractures may exist in the regions drilled in the PACMANUS hydrothermal field, but the low core recovery and fractured nature of the recovered core made it impossible to determine the amount of fractures from core analyses. However, recovered portions of the core were often brecciated or fractured. Additionally, preliminary downhole logging results indicate that there are a significant number of fractures and brecciated zones (Binns, Barriga, Miller, et al., 2002; Bartetzko et al., 2003) that may serve as conduits for hydrothermal fluid circulation. Future work is still in progress to determine fracture aperture and density parameters and their importance to the PACMANUS system.

CONCLUSIONS

Here we present the first permeability data from an actively venting, felsic hydrothermal environment. The variability in the data set is large, spanning five orders of magnitude. The variability could be because of micro-fracturing within the core samples, varying amounts or types of alteration that has taken place in a particular sample, or other heterogeneities that are not readily apparent in thin section analysis. Permeability decreases with depth, with near-surface values ranging from 10^{-17} to 10^{-15} m^2 and deeper values ranging from 10^{-19} to 10^{-15} m^2. Permeability also decreases with decreasing porosity. When the amount of alteration is considered, trends between both porosity and permeability with depth are more apparent. Completely altered samples decrease in both permeability and porosity as depth increases. Less altered samples re-

tain a relatively constant permeability and porosity, with several outlying values. Correlations to other physical properties such as velocity or thermal conductivity are not readily apparent.

The average permeability of the PACMANUS hydrothermal field is higher than measured permeabilities in other seafloor environments, based on similar laboratory measurements. The cause for this elevated permeability is undetermined; however, it may be related to the felsic nature of the rock or alteration features, both defining characteristics of the minicore samples. In situ permeabilities would likely be greater than values measured in the laboratory tests because of macro-scale fracturing, which would serve as flow conduits. Fluid flow velocities observed in the PACMANUS hydrothermal vents are larger than could be obtained from rocks with a bulk permeability of 10^{-16} m^2 as computed by simplified analytical calculations. Also, permeability values for each site do not correspond to observed differences in surface flow velocities. For example, Site 1189, which has rapid, focused venting, does not have a higher average permeability than Site 1188, which exhibits slow, diffusive venting. Therefore, the fluid flow processes in the basin are likely to be strongly influenced by the large-scale faulting and macro-scale fracturing. Future analysis of the fracture field based on logging information together with these core-scale data can be used to further establish the permeability field in the PACMANUS hydrothermal field.

ACKNOWLEDGMENTS

The authors would like to thank the ODP technical staff and the crew of the *JOIDES Resolution* for their hard work during Leg 193. We are also grateful to Wolfgang Bach at Woods Hole Oceanographic Institute for conducting fluid analyses. The authors are grateful to Ray Binns, Stuart Barclay, and Richard Wordon for insightful comments that greatly improved this manuscript. This research used samples and data provided by the Ocean Drilling Program (ODP). ODP is sponsored by the U.S. National Science Foundation (NSF) and participating countries under the management of Joint Oceanographic Institutions (JOI), Inc. Funding for this research was provided by a grant from the U.S. Science Support Program, award numbers F001396 and F001344.

REFERENCES

Bartetzko, A., Paulick, H., Iturrino, G., and Arnold, J., 2003. Facies reconstruction of a hydrothermally altered dacite extrusive sequence: evidence from geophysical downhole logging data (ODP Leg 193). *Geochem., Geophys., Geosyst.,* 4:10.1029/2003GC000575.

Becker, K., Morin, R.H., and Davis, E.E., 1994. Permeabilities in the Middle Valley hydrothermal system measured with packer and flowmeter experiments. *In* Mottl, M.J., Davis, E.E., Fisher, A.T., and Slack, J.F. (Eds.), *Proc. ODP, Sci. Results,* 139: College Station, TX (Ocean Drilling Program), 613–626.

Binns, R.A., Barriga, F.J.A.S., Miller, D.J., et al., 2002. *Proc. ODP, Init. Repts.,* 193 [CD-ROM]. Available from: Ocean Drilling Program, Texas A&M University, College Station TX 77845-9547, USA.

Binns, R.A., Parr, J.M., Scott, S.D., Gemmell, J.B., and Herzig, P.M., 1995. PACMANUS: an active seafloor hydrothermal field on siliceous volcanic rocks in the Eastern Manus Basin, Papua New Guinea. *In* Mauk, J.L., and St. George, J.D. (Eds.), *Proc. 1995 Pac. Rim Congress,* Australas. Inst. Min. Metall., Melbourne, 49–54.

Binns, R.A., and Scott, S.D., 1993. Actively forming polymetallic sulfide deposits associated with felsic volcanic rocks in the eastern Manus back-arc basin, Papua New Guinea. *Econ. Geol.,* 88:2226–2236.

Boitnott, G.N., 1997. Use of complex pore pressure transients to measure permeability of rocks. *Pap. Conf.—Soc. Pet. Eng. AIME,* 38717:37–45.

Christensen, N.I., and Ramananantoandro, R., 1988. Permeability of the oceanic crust based on experimental studies of basalt permeability at elevated pressures. *Tectonophysics,* 149:181–186.

Domenico, P.A., and Schwartz, F.W., 1997. *Physical and Chemical Hydrogeology* (2nd ed.): New York (Wiley).

Fisher, A.T., 1998. Permeability within basaltic oceanic crust. *Rev. Geophys.,* 36:143–182.

Iturrino, G.J., Davis, E., Johnson, J., Gröschel-Becker, H., Lewis, T., Chapman, D., and Cermak, V., 2000. Permeability, electrical, and thermal properties of sulfide, sedimentary, and basaltic units from the Bent Hill area of Middle Valley, Juan de Fuca Ridge. *In* Zierenberg, R.A., Fouquet, Y., Miller, D.J., and Normark, W.R. (Eds.), *Proc. ODP, Sci. Results,* 169, 1–42 [CD-ROM]. Available from: Ocean Drilling Program, Texas A&M University, College Station TX 77845-9547, USA.

Johnson, D.M., 1980. Fluid permeability of oceanic basalts. *In* Donnelly, T., Francheteau, J., Bryan, W., Robinson, P., Flower, M., Salisbury, M., et al., *Init. Repts. DSDP,* 51, 52, 53 (Pt. 2): Washington (U.S. Govt. Printing Office), 1473–1477.

Karato, S., 1983a. Physical properties of basalts from Deep Sea Drilling Project Hole 504B, Costa Rica Rift. *In* Cann, J.R., Langseth, M.G., Honnorez, J., Von Herzen, R.P., White, S.M., et al., *Init. Repts. DSDP,* 69: Washington (U.S. Govt. Printing Office), 687–695.

Karato, S., 1983b. Physical properties of basalts from the Galapagos, Leg 70. *In* Honnorez, J., Von Herzen, R.P. et al., *Init. Repts. DSDP,* 70: Washington (U.S. Govt. Printing Office), 423–428.

Yang, K., and Scott, S.D., 1996. Possible contribution of a metal-rich magmatic fluid to a sea-floor hydrothermal system. *Nature,* 383:420–423.

Figure F1. Location of the PACMANUS hydrothermal field in the Manus Basin, northeast of Papua New Guinea (after Binns et al., 1995).

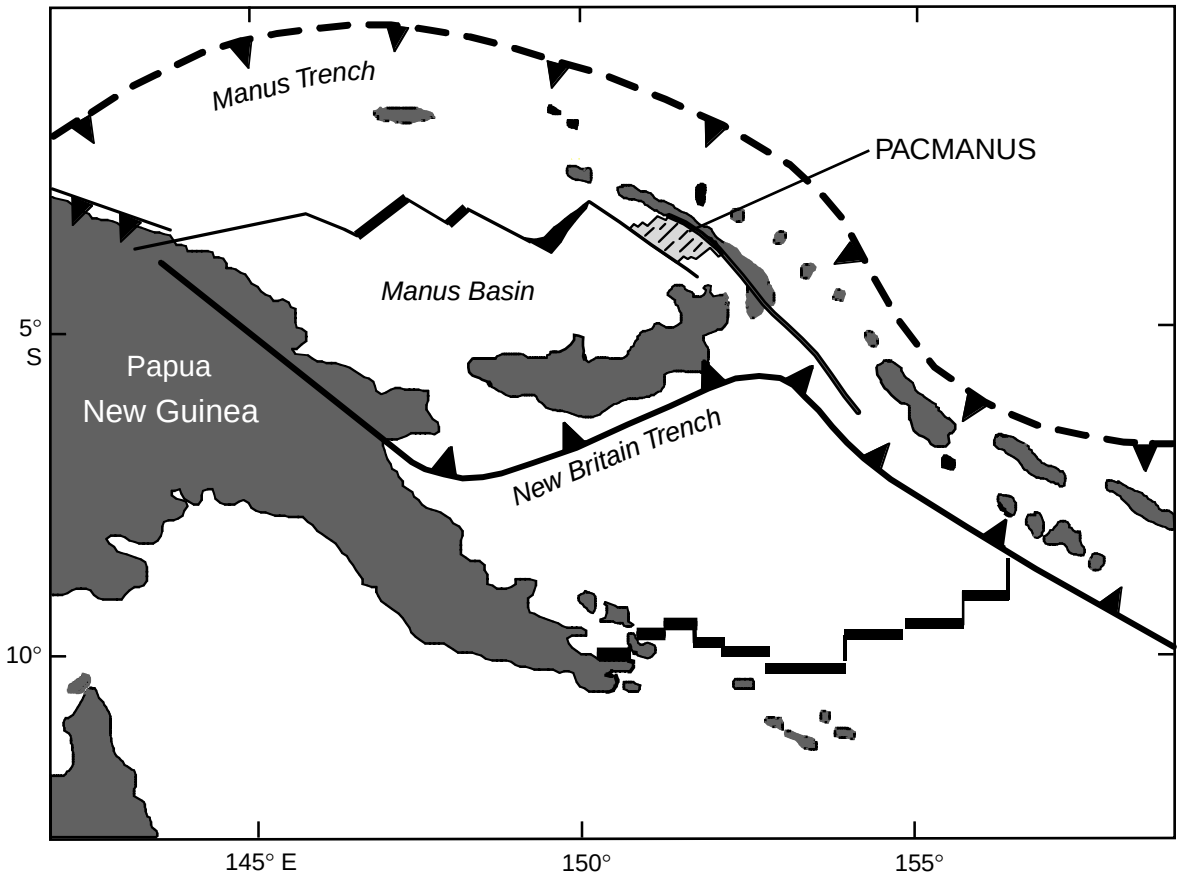

Figure F2. Permeability measurements as a function of confining pressure for samples with little response to pressure, increasing from a confining pressure of ~5 MPa to ~50 MPa and then decreasing to 5MPa. * = samples damaged during the permeability test.

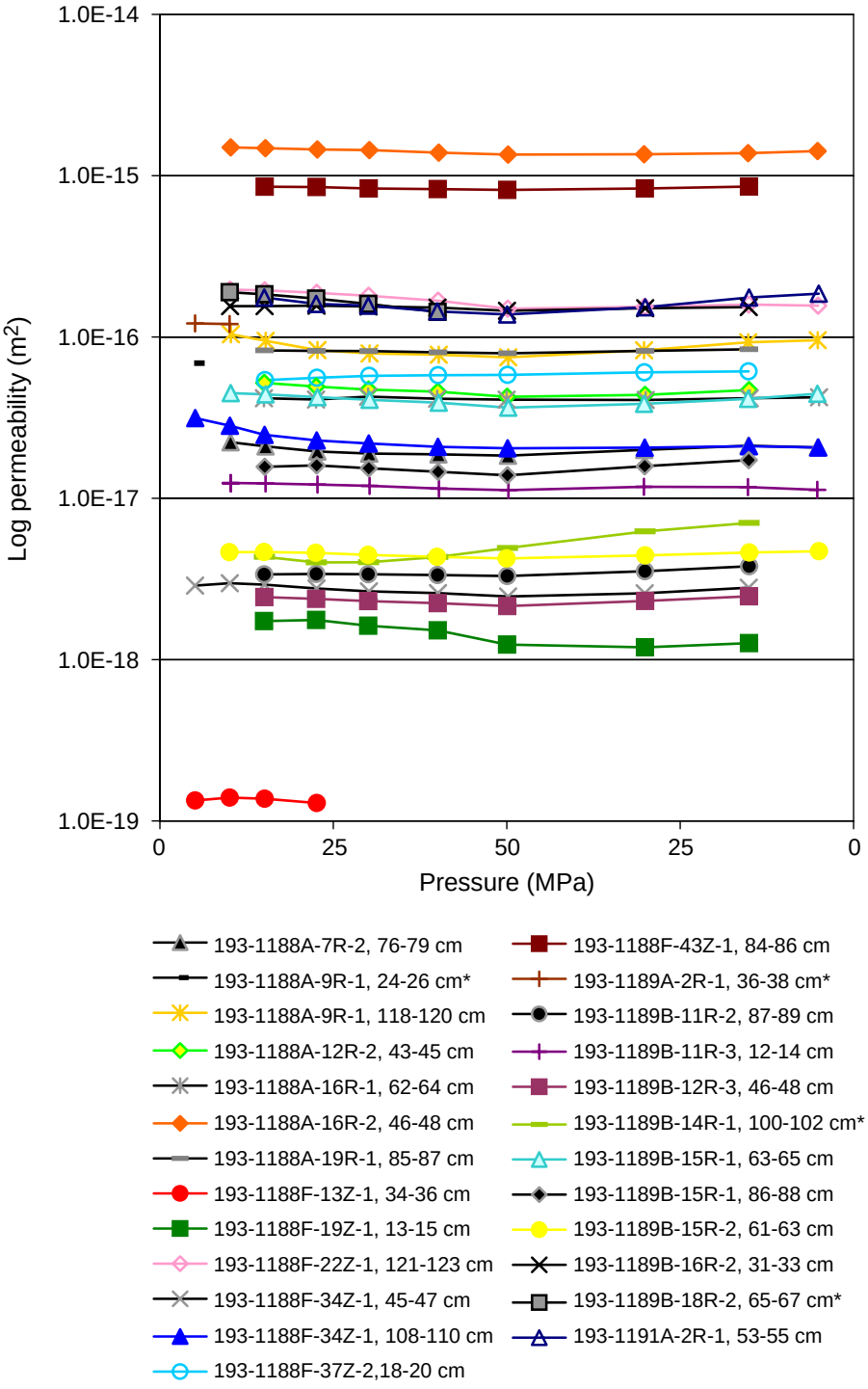

Figure F3. Permeability measurements as a function of confining pressure for samples with a large response to pressure, increasing from a confining pressure of ~5 MPa to ~50 MPa and then decreasing to 5MPa. * = samples damaged during the permeability test.

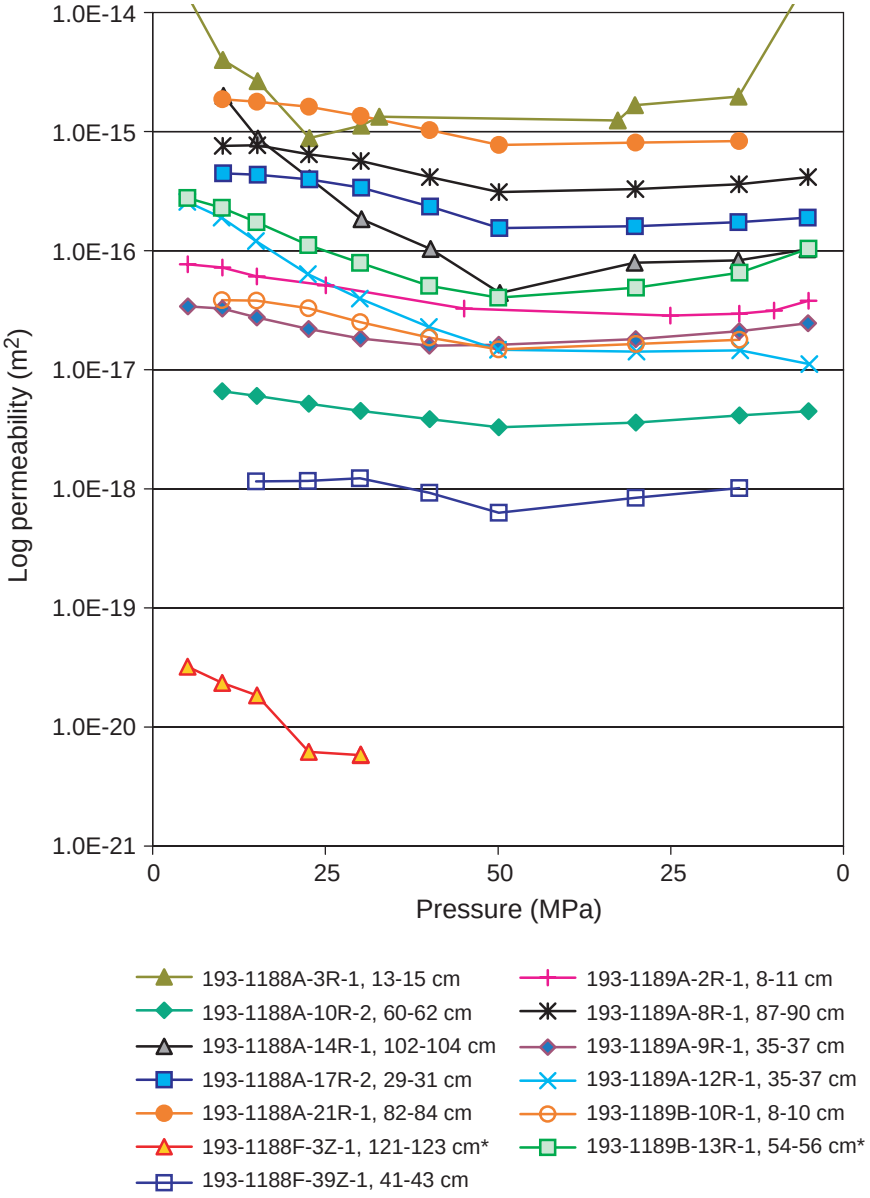

Figure F4. Core-scale permeability vs. depth. X = permeability measurements that are not considered reliable because of failure during testing.

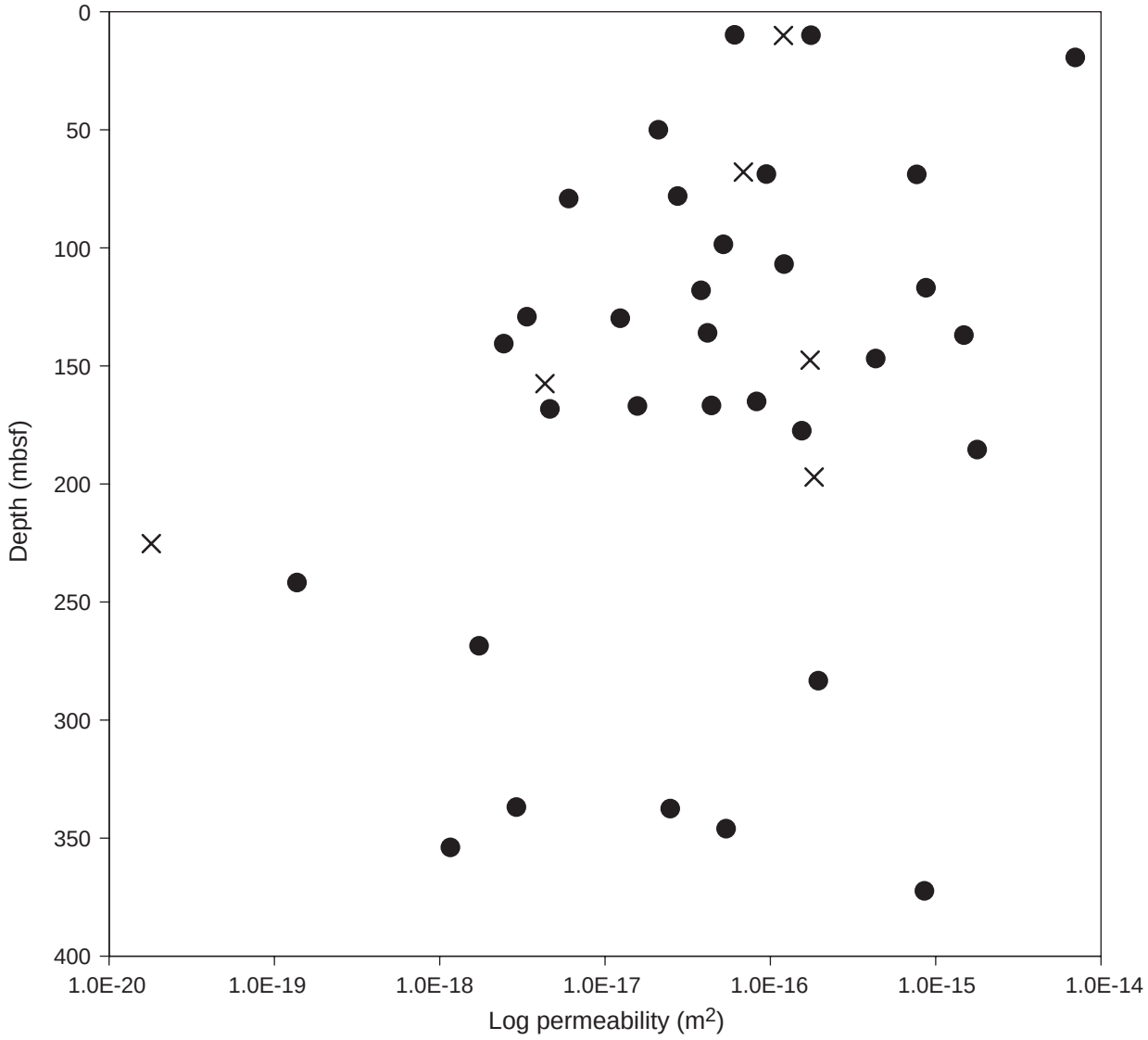

Figure F5. Core-scale permeability vs. porosity. Solid symbols = shipboard measurements during Leg 193; open symbols = measurements made at New England Research, Inc. (NER). X = permeability measurements that are not considered reliable because of failure during testing.

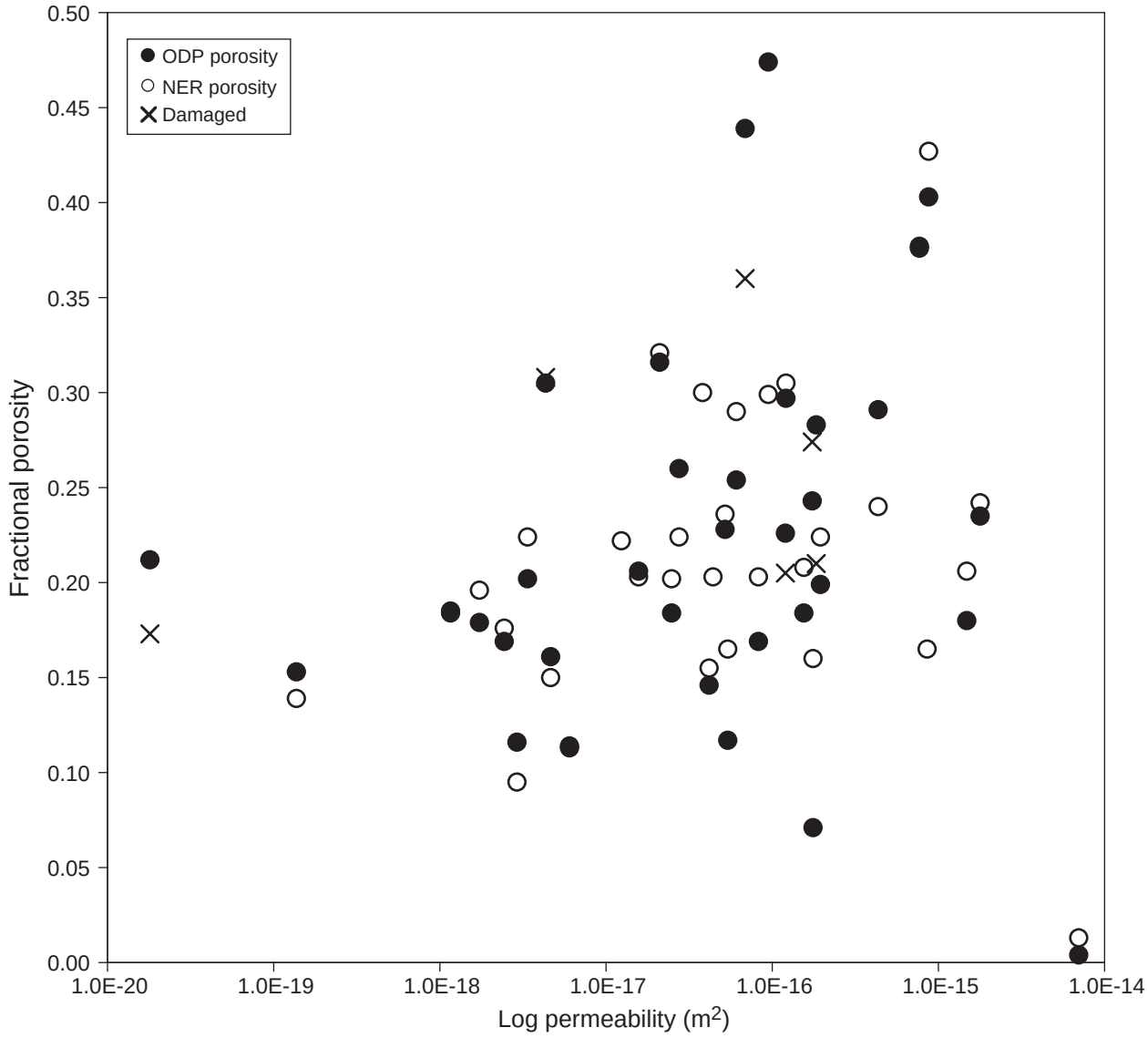

Figure F6. Porosity and permeability vs. depth for samples, dependent upon amount of alteration. Fresh refers to relict plagioclase, pyroxene, and glass. X = permeability measurements that are not considered reliable because of failure during testing. **A.** Porosity vs. depth for samples with >5% fresh rock. Solid circles = >20% fresh rock (termed highly altered in text); open circles = 5%–20% fresh rock (termed very highly altered in text). **B.** Porosity vs. depth for samples with <5% fresh rock (termed completely altered in text). **C.** Permeability vs. depth for samples with >5% fresh rock. Solid circles = >20% fresh rock; open circles = 5%–20% fresh rock. **D.** Permeability vs. depth for samples with <5% fresh rock.

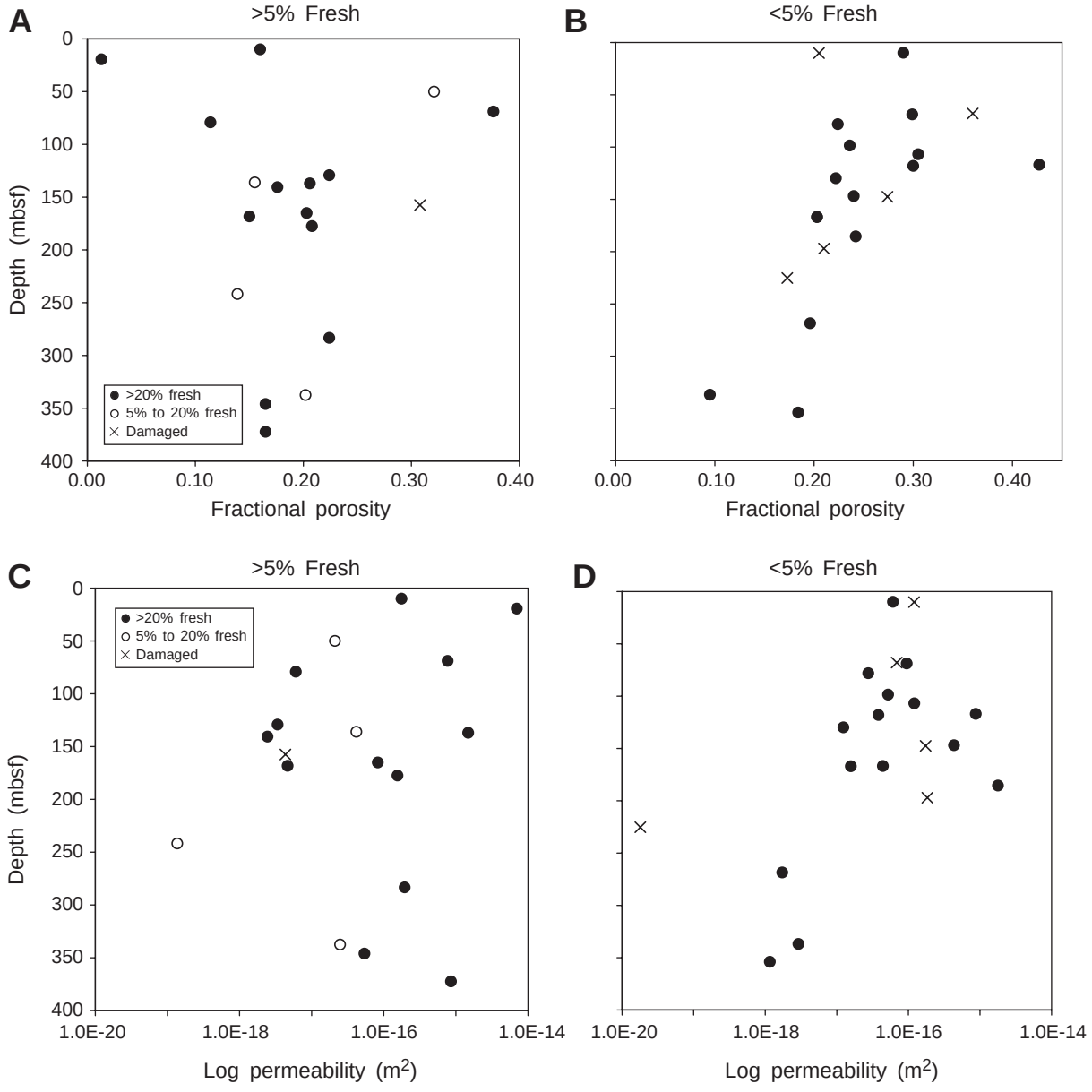

Figure F7. Porosity vs. permeability for samples with (**A**) >5% fresh rock and (**B**) <5% fresh rock. Solid circles = >20% fresh rock; open circles = 5%–20% fresh rock. X = permeability measurements that are not considered reliable because of failure during testing. Samples that have <5% fresh rock have a linear correlation between permeability and porosity, whereas samples with >5% fresh rock are less well correlated.

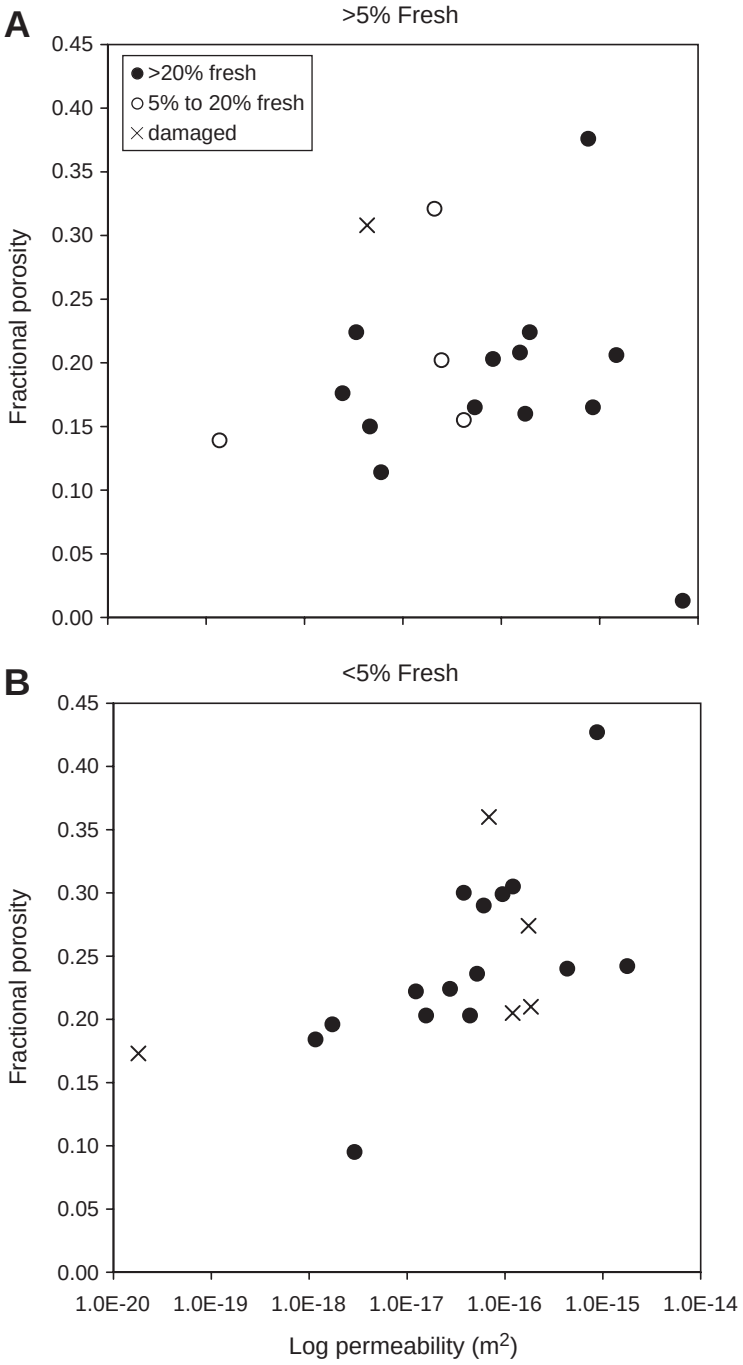

Figure F8. Comparison of core-scale permeability in the PACMANUS hydrothermal field to other submarine environments. Data from: southwest Bermuda Rise, Johnson, 1980; Costa Rica Rift, Karato, 1983a; Tonga-Kermadec and Juan de Fuca (solid symbols), Christensen and Ramananantoandro, 1988; Galapagos, Karato, 1983b; Juan de Fuca (open symbols), Iturrino et al., 2000.

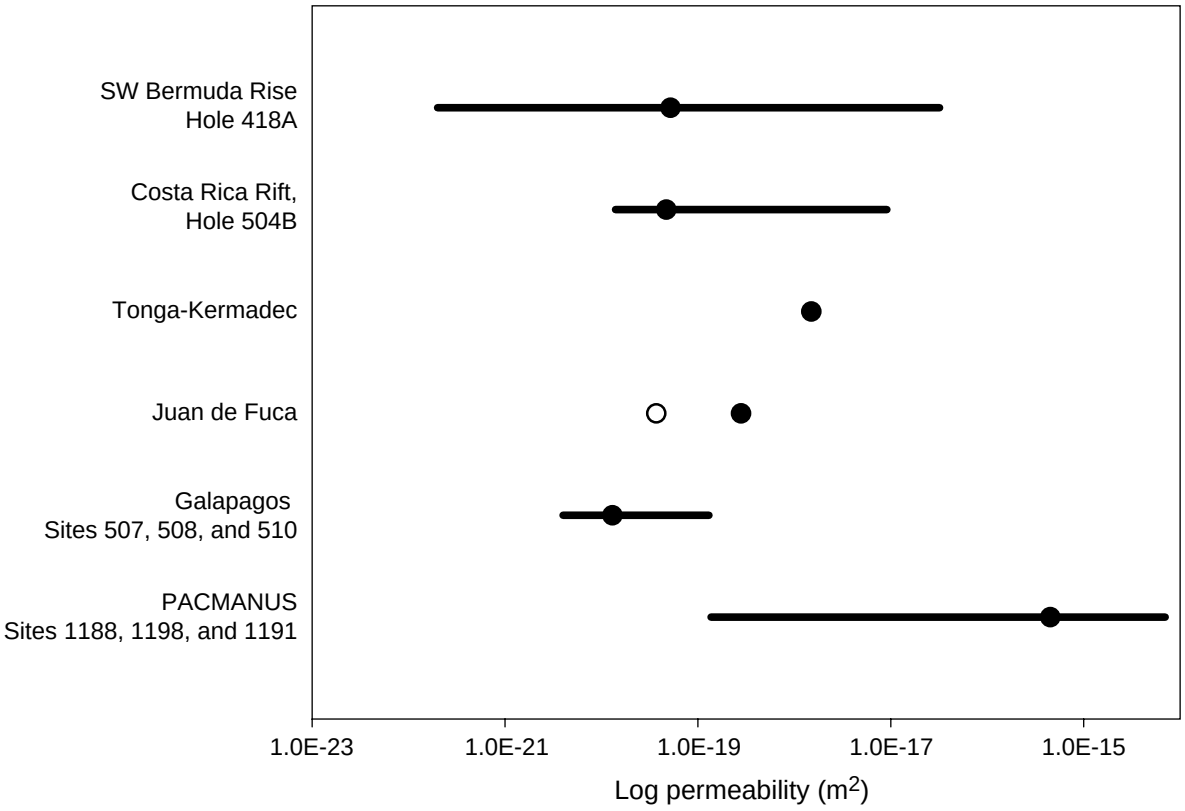

Table T1. Physical properties of samples from the PACMANUS hydrothermal field.

Core, section, interval (cm)	Piece	Current depth (mbsf)	Unit	Permeability (m^2)	ϕ (NER) (%)	ϕ (ODP) (%)	Vesicles (%)	Velocity (km/s)	Minerals (%)						Alteration intensity	Comments
									Fresh	Anhydrite	Quartz	Silica/ Cristobalite	Clay	Sulfide		
193-1188A-																
3R-1, 13–15		19.36	1	6.99E–15	0.013	0.004	10				0				Fresh	
7R-2, 76–79	6	49.98	6	2.10E–17	0.321	0.316	Trace	3.5							Very high	
9R-1, 24–26	4	67.90	7	6.87E–17	0.360	0.439	5								Complete	Damaged during testing
9R-1, 118–120	9	68.75	8	9.47E–17	0.299	0.474									Complete	
10R-2, 60–62	10	79.11	9	6.03E–18	0.114	0.113	Trace	4.7							High	
12R-2, 43–45	4	98.51	10	5.20E–17	0.236	0.228		3.6							Complete	
14R-1, 102–104	14	116.90	14	8.74E–16	0.427	0.403				16	42	21	21	Trace	Complete	1 cm from thin section
16R-1, 62–64	9	136.01	17	4.17E–17	0.155	0.146	3	4.6							Very high	
16R-2, 46–48	7	136.95	18	1.48E–15	0.206	0.180	Trace	3.9	37		42		15	6	High	3 cm from thin section
17R-2, 29–31	6	146.87	19	4.34E–16	0.240	0.291		4.4		20	55		20	5	Complete	2 cm from thin section
19R-1, 85–87	16	165.05	22	8.26E–17	0.203	0.169	5	3.8							High	
21R-1, 82–84	10	185.43	25	1.78E–15	0.242	0.235	0								Complete	
193-1188F-																
3Z-2, 121–123	2C	225.27	30	1.80E–20	0.173	0.212	0			5	65		29	1	Complete	Damaged during testing
13Z-1, 34–36	2A	241.75	39	1.37E–19	0.139	0.153	0	4.5	7	1	40		50	2	Very high	
19Z-1, 13–15	1B	268.54	45	1.73E–18	0.196	0.179	0	4.8		2	26		67	5	Complete	
22Z-1, 121–123	15	283.32	46	1.95E–16	0.224	0.199			40	2	25		30	3	High	
34Z-1, 45–47	9	336.86	55	2.91E–18	0.095	0.116	2				57		40	3	Complete	
34Z-1, 108–110	14	337.49	56	2.48E–17	0.202	0.184	0		7		60		32	1	Very high	
37Z-2, 18–20	2	346.00	57	5.40E–17	0.165	0.117	1	6.3	20		45		30	5	High	
39Z-1, 41–43	6	353.92	62	1.16E–18	0.184	0.185	3	4.0		1	60		39	Trace	Complete	
43Z-1, 84–86	3C	372.34	72	8.55E–16	0.165	NA	5		26	2	40		29	3	High	1 cm from thin section
193-1189A-																
2R-1, 8–11	2	9.78	2	6.08E–17	0.290	0.254	15	3.8							Complete	
2R-1, 36–38	6	10.07	2	1.20E–16	0.205	0.226	7	3.5							Complete	Damaged during testing
8R-1, 87–90	14	68.88	15	7.69E–16	0.376	0.377			41		3		55	1	High	Adjacent to thin section
9R-1, 35–37	5	78.06	16	2.75E–17	0.224	0.260									Complete	
12R-1, 35–37	5	106.86	20	1.21E–16	0.305	0.297	5								Complete	
193-1189B-																
10R-1, 8–10	1	117.99	13	3.81E–17	0.300	NA	10								Complete	
11R-2, 87–89	8	129.16	19	3.37E–18	0.224	0.202	8	3.9	35		5	35	25		High	Adjacent to thin section
11R-3, 12–14		129.81	19	1.24E–17	0.222	NA									Complete	
12R-3, 46–48	7	140.56	19	2.44E–18	0.176	0.169	10	4.0	20		2	38	40		High	
13R-1, 54–56	10	147.55	21	1.74E–16	0.274	0.243	5	4.6			50		49	1	Complete	Damaged during testing/adjacent to thin section
14R-1, 100–102	14	157.51	23	4.33E–18	0.308	0.305			55	4	31		5	1	High	Damaged during testing
15R-1, 63–65	9A	166.74	25	4.40E–17	0.203	NA									Complete	
15R-1, 86–88	11	166.97	25	1.57E–17	0.203	0.206		4.7	5		5	10	80		Complete	
15R-2, 61–63	10	168.21	26	4.64E–18	0.150	0.161		4.9	42		13	35	10		High	
16R-2, 31–33	4	177.44	27	1.55E–16	0.208	0.184	5	4.9	20		50		30		High	
18R-2, 65–67	8	197.08	35	1.84E–16	0.210	0.283			3		35	46	15	1	Complete	Damaged during testing
193-1191A-																
2R-1, 53–55	8	9.93	1	1.76E–16	0.160	0.071	Trace	5.6							Slight	

Notes: Minerals come from thin section analyses (Binns, Barriga, Miller, et al., 2002). ϕ = porosity. Alteration intensity classifications: fresh = <2% alteration, slight = 2%–10%, high = 40%–80%, very high = 80%–95%, complete = 95%–100%. NA = not available.